Structural Investigation of the Binding of Nucleotide to Phosphoenolpyruvate Carboxykinase by NMR†

Todd Holyoak§ and Thomas Nowak*

Department of Chemistry and Biochemistry, University of Notre Dame, Notre Dame, Indiana 46556

Received June 29, 2001

ABSTRACT: The enzyme phosphoenolpyruvate carboxykinase (PEPCK) catalyzes the reversible conversion of oxalacetate and GTP to phosphoenolpyruvate (PEP), GDP, and CO_2. PEPCK from higher organisms is a monomer, specifically requires GTP or ITP, and uses Mn^{2+} as the activating cation. Currently, there is no crystal structure of GTP-utilizing PEPCKs. The conformation of the bound nucleotide was determined from transferred nuclear Overhauser effects (trnOe) experiments to determine internuclear proton distances. At 600 MHz in the presence of PEPCK, nOe effects were observed between nucleotide protons. Internuclear distances were calculated from the initial rate of the nOe buildup. These distance constraints were used in energy minimization calculations to determine the conformation of PEPCK-bound GTP. The bound nucleotide has the base oriented anti to the $C_{2'}$-endo(^{2}E) ribose ring conformation. Relaxation rate studies indicate that there is an additional relaxation effect on the $C_{1'}$ proton upon nucleotide binding to PEPCK. Nucleotide binding to PEPCK−Mn^{2+} was studied by ^{1}H relaxation rate studies, but results were complicated by long dipole−dipole distances and the presence of competing complexes. Modification of PEPCK by iodoacetamido-TEMPO leads to an inactive enzyme that is spin-labeled at cys273. The interaction of TEMPO−PEPCK with GTP allows for the measurement of nuclear distances between GTP and the spin label. The results suggest that cys273 lies near the ribose ring of the bound nucleotide, but it is too far to be implicated in direct hydrogen bonding interactions consistent with previous results [Makinen, A. L., and Nowak, T. *J. Biol. Chem*. (1989) *264*, 12148], suggesting that cys273 does not actively participate in catalysis. Modification of PEPCK with several cysteine specific modifying agents causes no change in the ability of the enzyme to bind nucleotide as monitored by fluorescence quenching. A correlation between the size of the modifying agent and the maximal observed quenching upon saturation of the enzyme with nucleotide is observed. This suggests a mechanism for inactivation of PEPCK by cysteine modification due to inhibition of a dynamic motion that may occur upon nucleotide binding.

Phosphoenolpyruvate carboxykinase [GTP/ITP: oxaloacetate carboxylase (trans-phosphorylating, EC 4.1.1.32)] (PEPCK)[1] catalyzes the reversible decarboxylation of oxaloacetic acid with the concomitant transfer of the γ-phosphate of GTP (or ITP) to form PEP and GDP (IDP) as illustrated in Scheme 1. The primary role of the enzyme is the formation of PEP in the first committed step of gluconeogenesis (*1*). This has led to the suggestion of PEPCK as a potential target for drug therapy in humans in the treatment of noninsulin-dependent diabetes (*2*). The enzyme isoform isolated from chicken liver mitochondria has been shown to be a monomeric protein of 67 kDa (*3*). PEPCK has been isolated and studied from a variety of sources. PEPCK occurs in the cytosol of the adult rat, mouse, and hamster liver (*4*) and in the mitochondria of adult pigeon and chicken liver (*5*, *6*). PEPCK occurs in both the cytosol and mitochondria in rabbit, pig, and human liver (*4*, *7*−*9*). The cytosolic and mitochondrial forms are distinct gene products and can be distinguished from each other biochemically. The primary sequences of the GTP class of PEPCK from several sources have been elucidated and are found to contain approximately 60−65% identity among all sources. An additional class of PEPCK exists in bacteria, yeast, and other lower organisms. Two of the best studied isozymes from this class are yeast PEPCK, a functional tetramer, and *Escherichia coli* PEPCK, a monomer that

Scheme 1

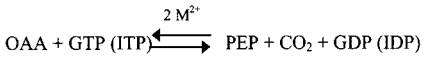

† This research was supported in part by a grant from the National Institutes of Health (DK17049) to T.N. and by the Department of Chemistry & Biochemistry, University of Notre Dame.

* To whom correspondence should be addressed at The Department of Chemistry and Biochemistry, University of Notre Dame, Notre Dame, IN 46556; (219) 631-5859; Fax (219) 631-3567; E-mail: Nowak.1@nd.edu.

§ Current address: Rosensthiel Basic Medical Sciences Research Center, Floor Six, Brandeis University, Mail Stop 029, 415 South Street, Waltham, MA 02454.

[1] Abbreviations: ATP, adenosine-5′-triphosphate; DTNB, 5,5′-dithiobis (2-nitrobenzoic acid); DTT, 1,4-dithiothreitol; EPR, electron paramagnetic resonance; GDP, guanosine-5′-diphosphate; GMP, guanosine-5′-monophosphate; GTP, guanosine-5′-triphosphate; GST, glutathione-*S*-transferase; IDP, inosine-5′-diphosphate; ITP, inosine-5′-triphosphate; MDH, malate dehydrogenase; MMTS, methyl methanethiosulfonate; NADH, nicotinamide adenine dinucleotide, reduced form; NMR, nuclear magnetic resonance; OAA, oxaloacetic acid; PEP, phosphoenolpyruvate; cPEPCK, rat cytosolic phosphoenolpyruvate carboxykinase; mPEPCK, avian mitochondrial phosphoenolpyruvate carboxykinase; PRR, water proton longitudinal relaxation rate; nOe, nuclear Overhauser effect; trnOe, transferred nuclear Overhauser effect.

10.1021/bi011374n CCC: $20.00
Published on Web 08/22/2001

exhibits kinetic cooperativity. These enzymes utilize ATP rather than GTP (ITP) as the phosphoryl donor. While *E. coli* PEPCK is monomeric, a majority of enzymes in this group are multimers. These enzyme forms have been found to have relatively low overall identity with the GTP-utilizing class of enzymes but do exhibit conservation of some proposed active site residues.

At the present time, little structural information on the chicken mitochondrial form, and on any of the GTP-utilizing class of PEPCKs, has been elucidated. The nucleotide and subsequently derived protein sequence of the mitochondrial isozyme of the chicken liver form of the enzyme has previously been determined (*3*); however, no crystallographic data exist on this or any other GTP-utilizing PEPCK forms. The crystal structure of the *E. coli* form of the enzyme has been solved (*10*−*12*). In this structure, the bound ATP is shown to be in a *syn*-conformation, which is unusual for ATP (*11*, *12*). These same authors have proposed a general nucleotide binding sequence for all PEPCK isoforms based on their structural data and sequence alignments (*11*). If this is true, one may expect a similar nucleotide conformation in the GTP-utilizing class of enzymes. Previous studies on PEPCK have elucidated structural information based on NMR relaxation rate methods (*13*−*15*). These studies have offered geometric constraints on PEP and nucleotide structures relative to the activating cation (Mn^{2+}). The distance of a reactive cysteine residue relative to nucleotide phosphates and the activating metal was also determined by the use of a spin-labeled enzyme and by EPR and NMR spectroscopy (*15*). This research was undertaken to elucidate the conformation of the bound nucleotide by trnOe and to provide further geometric constraints through relaxation rate studies on the nucleotide protons. These results will yield additional structural information regarding the substrates at the active site of the enzyme in the absence of crystallographic data and lend insight into the reaction catalyzed by the GTP-utilizing isoforms of PEPCK.

MATERIALS AND METHODS

Materials. All materials used were of the highest purity commercially available. All materials used for proton NMR (Tris, KCl, $MgCl_2$, $MnCl_2$, and GTP) were exchanged into D_2O by multiple lyophilization cycles prior to use. All the solutions, except for metals, were treated with Chelex resin (Bio-Rad) to remove any contaminating metal species.

mPEPCK Purification. PEPCK was isolated as previously reported (*13*). Protein concentration was determined from the A_{280} and an extinction coefficient of $\epsilon_{280} = 16.5 \pm 0.1$ $(mg/mL)^{-1}$ and a molecular mass of 67 000 Da (*3*, *16*).

cPEPCK Purification. The gene for rat cPEPCK was provided as a generous gift from Dr. H. Yoo-Warren at Bayer Laboratories. This gene exists as a fusion construct with glutathione *S*-transferase in the pGEX-4T-2 vector (Pharmacia). Overnight cultures of BL-21 *E. coli* cells (Invitrogen) that had been transformed with the vector were diluted 10-fold and grown at 37 °C until the OD_{600} reached 0.7−1.0. The cells were subsequently induced with 1 mM IPTG and grown for an additional 4−6 h. Cells were harvested and resuspended in buffer (50 mM Tris, 0.1 mM EDTA, 0.1 mM DTT) and lysed by French press. The cell debris was pelleted by centrifugation at 9500 rpm for 15 min at 5 °C. The resultant supernatant was loaded onto glutathione-Sepharose (Agarose) and washed with 10 column volumes of buffer (50 mM Tris, 0.1 mM EDTA, 0.1 mM DTT, 1% NP-40, pH 7.0). The resin was then washed with 10 column volumes of 50 mM Tris, 0.1 mM EDTA, 0.1 mM DTT, pH 7.0, or until the A_{280} was less than 0.1. The fusion protein is designed such that a thrombin site exists between GST and cPEPCK. cPEPCK is removed from the glutathione resin by 6-h treatment with thrombin at 4 °C. The resin is washed with 5 column volumes of buffer. The washes are concentrated and the cPEPCK stored in 50 mM Tris, 0.1 mM EDTA, 0.1 mM DTT, 10% glycerol at 4 °C. This results in cPEPCK that is >95% pure and has an activity of 4−6 U mg^{-1} as assayed by the method outlined below. The purified cPEPCK is unstable and readily loses activity. PEPCK with activity less than 3 U mg^{-1} was not used in the experiments. Protein concentration was determined with the Bio-Rad protein assay kit (Bio-Rad).

PEPCK Assay. The carboxylation of PEP to form OAA, catalyzed by PEPCK, was assayed by the method of Hebda and Nowak (*16*). In this continuous assay, PEPCK is coupled to MDH and the disappearance of NADH is continuously monitored with time at 340 nm on a Gilford 240 or 250 spectrophotometer kept at 25 °C.

^1H and ^{31}P NMR. Data were collected on either a two-channel Varian VXR-500 spectrometer operating at a magnetic field strength of 11.7 T or a three-channel Varian Unity Plus spectrometer operating at a magnetic field strength of 14.1 T (600 MHz) equipped with waveform generators on all three channels and a z-gradient pulse field accessory. For ^1H NMR experiments, PEPCK was desalted on a P6DG gel filtration column (Bio-Rad) that was equilibrated in 10 mM Tris, pD 7.4, in D_2O. The enzyme was subsequently concentrated under nitrogen and diluted in 10 mM Tris, pD 7.4, and concentrated again. This was repeated several times to exchange a majority of the H_2O for D_2O. For ^{31}P experiments, PEPCK was desalted in a similar fashion with the exception that the P6DG column was equilibrated in 50 mM Tris pH 7.4 in H_2O.

The samples used for T_1 experiments contained between 150 and 180 μM enzyme, 100 mM KCl and either 6 mM GTP or 4 mM GMP. The longitudinal relaxation rate $1/T_1$ was plotted as a function of added Mn^{2+} concentration. The paramagnetic contribution to the relaxation rate, $1/T_{1p}$, was calculated from the difference in relaxation rates between samples with added Mn^{2+} and those without. This value was normalized by the factor p where $p = [Mn^{2+}_{bound}]/[ligand]$ to generate values of $1/pT_{1p}$. The concentration of Mn^{2+} bound to PEPCK was determined utilizing the K_D for Mn^{2+} of 40 μM. Under conditions of fast exchange $1/pT_{1p} = 1/T_{1M}$. The correlation time for the binary Mn-GTP complex was assumed to be that of the rotational correlation time (τ_r) and was estimated to be 0.1 ns. The same value was obtained either by using the previous calculations (*17*) or by assuming that τ_r is directly proportional to the mass of the GTP−Mn−$(H_2O)_4$ complex relative to $\tau_r = 2.9 \times 10^{-11}$ s for $Mn(H_2O)_6$. The correlation time in the presence of PEPCK was determined from the frequency dependence of the longitudinal relaxation rates. This is calculated using the dipolar term of the Solomon−Bloembergen equation (*18*, *19*). From the frequency dependence of the relaxation rates and assum-

ing τ_c is frequency independent, eq 1 can be used to calculate τ_c.

$$T_{1M(\nu 2)}/T_{1M(\nu 1)} = (1 + \omega_{I(\nu 2)}{}^2\tau_c{}^2)/(1 + \omega_{I(\nu 1)}{}^2\tau_c{}^2) \quad (1)$$

In eq 1, ω_I is the resonance frequency at each field, ν_1 and ν_2. The longitudinal relaxation rates of the nuclei can then be used in the Solomon−Bloembergen equation to calculate the distances between the nuclei and the paramagnetic center, utilizing the dipolar correlation time, τ_c. The simplified form of the equation becomes:

$$r\,(\text{Å}) = C[T_{1M}f(\tau_c)]^{1/6} \quad (2)$$

where C is a collection of constants. $C = 812$ for Mn-^{1}H, 601 for Mn-^{31}P and 539 for nitroxide−^{1}H interactions.

The correlation function $f(\tau_c)$ has the form:

$$f(\tau_c) = [(3\tau_c/1 + \omega_I{}^2\tau_c{}^2) + (7\tau_c/1 + \omega_s{}^2\tau_c{}^2)] \quad (3)$$

where ω_I and ω_s are the Larmor angular precession frequencies for the nuclear and electron spins and $\omega_s = 657\omega_I$. T_2 values were estimated from the line widths of the resonance signals at half-height by the equation:

$$1/T_2 = \pi(\nu - B) \quad (4)$$

where ν is the line width at half-height in Hertz, and B is the artificial line broadening. For the GMP−Mn−PEPCK complex, τ_c was determined from the ratio of the T_1/T_2 relaxation times. τ_c was calculated assuming only dipolar contributions of Mn^{2+} to the relaxation rates from the following equation:

$$\tau_c = [(6(T_{1M}/T_{2M}) - 7)/(4\omega_I{}^2)]^{1/2} \quad (5)$$

A more detailed treatment of the phenomena can be found in Nowak (*19*) and references therein.

Transferred nOe Experiments. nOe experiments were carried out at 600 MHz on a three-channel Varian Unity Plus spectrometer operating at a magnetic field strength of 14.1 T equipped with waveform generators on all three channels and a z-gradient pulse field accessory. The samples contained 10 mM Tris, pD 7.4, 4 mM GTP, 100 mM KCl, and either 249 or 180 μM mPEPCK or 190 μM cPEPCK in D_2O. This gave enzyme/GTP ratios of 1:16, 1:22, and 1:21, respectively. The enzyme samples were treated in an identical fashion as outlined for the T_1 experiments. The saturated resonance was inverted via a 40 μs selective Gaussian 180° pulse. This was followed by a delay time (τ_m) and a 90° pulse. An identical spectrum was obtained at each delay time where the 180° pulse was applied off resonance at 0 ppm. nOe effects were determined from the difference between the two spectra and the magnitude of the nOe is expressed as a percentage of the peak when irradiated at 0 ppm. The nOe intensity was obtained as a function of delay time τ_m. The delay times were varied from 25 to 500 ms.

The delay time and nOe intensity are related as shown in eq 6 (*20*):

$$I_{noe} = 1 - \exp(-R\tau_m) \quad (6)$$

which can also be written in expansion form as

$$I_{noe} = R\tau_m - (1/2)R^2\tau_m{}^2 + (1/6)R^3\tau_m{}^3 - \ldots$$

where R is the relaxation rate matrix that contains elements R_{ij}, that describe the initial rate of nOe buildup in a simple two-spin system consisting of protons H_i and H_j (*20*).

The initial buildup of nOe intensities were fit by eq 7.

$$I_{noe} = R_{ij}\tau_m - a_{ij}\tau_m{}^2 \quad (7)$$

In this equation, a_{ij} is a constant. To determine the internuclear distances, the method of ratio of slopes was used. It has been shown (*21*) that the internuclear distance between $H_{1'}$ and $H_{2'}$ of the ribose is 2.9 Å and is independent of nucleotide and ribose conformation. Using this value as an internal calibration standard, the other internuclear distances can be determined from eq 8.

$$r\,(\text{Å}) = [(R_{H1'-H2'}/R_{ij}) \times 2.9^6]^{1/6} \quad (8)$$

Molecular Modeling. Energy minimization of the conformation of bound GTP was performed using InsightII. The calculated distances from the nOe experiments were used as constraints. The distances were allowed to vary by 10%. Minimization was performed in a dielectric constant of 0.78 at 298 °K using a combination of steepest descent and conjugate gradients algorithms for 1000 iterations or until the RMS was < 0.001. From the final structure, internuclear distances as well as torsion angles were measured. The pseudorotation phase angle (P) is calculated from eq 9 (*21*).

$$P = \tan^{-1}[(\nu_4 + \nu_1 - \nu_3 - \nu_0)/2\nu_2(\sin 36° + \sin 72°)] \quad (9)$$

Preparation of Modified Forms of PEPCK. PEPCK was desalted on a P6DG column with a 1-cm layer of Chelex resin on the top, equilibrated in 50 mM Tris-HCl, pH 7.4. The enzyme was concentrated to 4 mg/mL in an Amicon nitrogen concentrator with a PM 30 membrane. The enzyme solution was degassed by bubbling a stream of N_2 gas through the solution. For modification of the enzyme with iodoacetamido-TEMPO, the enzyme was incubated with a 10% molar excess of iodoacetamido-TEMPO in the dark at 4 °C for a period of 10−16 h until the residual activity was <5% of the original activity. The enzyme was applied to a second P6DG/Chelex column, equilibrated with 10 mM Tris pH 7.4 in D_2O, and concentrated to 6 mg/mL. If the enzyme was not utilized in NMR studies, it was applied to a P6DG/Chelex column equilibrated in 50 mM Tris-HCl, pH 7.4, and concentrated as previously described. The other modified forms of the enzyme were synthesized as previously described (*15*); the only difference is that the MMTS modification was complete within 5 min.

Cysteine Determinations. Cysteine content of native and modified PEPCK forms was determined by the method of Habeeb (*22*). Approximately 1 nmol of PEPCK was incubated in a solution of 1 mM DTNB, 6 M guanidine HCl, and the absorbance at 412 nm was recorded. A blank solution containing all components except enzyme was used to correct the absorbance values obtained. The free cysteine concentration was determined using the reported extinction coefficient of 13 600 M^{-1} cm^{-1}. PEPCK concentrations were determined spectrophotometrically as previously described.

Table 1: Normalized Relaxation Rates of GTP Protons in the Binary Mn−GTP Complex[a]

nucleus	δ (ppm)	$1/pT_{1p}$ ($\times 10^3$ s^{-1})	τ_c (ns)[b]	R (Å)
$H_{1'}$	5.8	2.8 ± 0.2	0.1	5.51 ± 0.06
$H_{2'}$	4.7	12.9 ± 3.6	0.1	4.44 ± 0.17
$H_{3'}$	4.5	7.5 ± 1.0	0.1	4.68 ± 0.07
$H_{4'}$	4.2	21.6 ± 4.8	0.1	3.92 ± 0.13
$H_{5',5''}$	4.1	18.6 ± 2.0	0.1	4.02 ± 0.07
H_8	8.0	33.1 ± 1.9	0.1	3.65 ± 0.03
α-P[c]		23.6 ± 0.1	0.8	3.90 ± 0.05
β-P[c]		29.9 ± 0.2	0.8	3.75 ± 0.05
γ-P[c]		29.9 ± 0.1	0.8	3.75 ± 0.05

[a] Relaxation rates were determined at 500 MHz; distances from the nuclei to the metal were calculated from eqs 2 and 3. [b] τ_c determined from the molecular weight of the binary Mn−GTP complex. [c] ^{31}P data from Lee and Nowak (*13*) at 121.5 MHz.

Determination of Binding Constants for Nucleotides by Fluorescence. Fluorescence measurements were performed in a 1-cm path length cuvette containing PEPCK (5−10 μM), 100 mM KCl, and 50 mM Hepes, pH 7.4. Emission was monitored at 335 nm after excitation at 297 nm. The sample chamber was thermostatically controlled to 10 ± 0.1 °C. To determine binding constants for the nucleotides, the sample was titrated with an identical sample containing either GMP, GDP, GTP, or IDP. The binding constants and maximal quenching values were determined by a nonlinear least-squares fit to the titration data using the equation

$$Q = Q_{max}[L]/K_d + [L] \quad (10)$$

In eq 10, Q is the measured quenching of fluorescence, Q_{max} is the maximal quenching obtained, [L] is the concentration of nucleotide titrated into the sample of PEPCK, and K_d is the dissociation constant of the complex.

RESULTS

Paramagnetic Relaxation Effects on GMP and GTP. The proton NMR spectrum for GTP was obtained at 500 MHz as described in Materials and Methods, and the longitudinal relaxation rates ($1/T_1$) were measured. $MnCl_2$ was titrated into the sample and the effect of Mn^{2+} on the $1/T_1$ values of the nucleotide protons were determined. Plots of the observed $1/T_1$ versus Mn^{2+} were linear (data not shown). From the normalized relaxation rates ($1/pT_1p$) and utilizing a correlation time (τ_c) of 0.1×10^{-9} s^{-1}, the distances between the proton nuclei and the Mn^{2+} were calculated using eqs 2 and 3 (Table 1).

To determine the relative conformation and localization of the nucleotide when bound to PEPCK, the same experiment was performed in the presence of 180 μM PEPCK. Mn^{2+} was titrated into the solution, and the effect on the relaxation rates was determined. The plots of $1/T_1$ at 300 and 500 MHz versus Mn^{2+} concentration are linear with respect to the concentration of Mn^{2+} added (data not shown). The correlation time was obtained from the ratio of the $1/pT_{1p}$ relaxation rates at 300 and 500 MHz and was between 0.13 and 0.25 ns. The distances from the paramagnetic center to the protons of the nucleotide are calculated from the Solomon−Bloembergen equation using values of $1/pT_{1p}$ and τ_c from the titration experiments (Table 2). The Mn^{2+}-to-proton distances from this study are not significantly different from those calculated from the binary Mn^{2+}−GTP complex (Table 1). This could result from one of two possibilities. PEPCK binds GTP in the same conformation that exists in solution and the relative location of the bound Mn^{2+} is the same. Alternatively, even in the presence of enzyme, the complex being measured could primarily be that of the binary Mn^{2+}−GTP complex. The latter case appears to be the explanation as reflected by the extremely short correlation times that are calculated in the presence of enzyme from the frequency dependence of the relaxation rates. Thus, the excess of nucleotide over enzyme is sufficient to ensure that the binary Mn^{2+}−GTP complex is the predominant species in solution that influences the relaxation rate effects. In an attempt to overcome the ability of GTP to chelate the Mn^{2+}, the experiment was repeated in the presence of 4 mM GTP and 8 mM $MgCl_2$. This experiment was performed in an attempt to have Mg^{2+} compete against Mn^{2+} binding to free GTP. Mg^{2+} binds to PEPCK 3 orders of magnitude more weakly than does Mn^{2+} (*23*). The results obtained were not significantly different from those obtained in the experiment without Mg^{2+} (data not shown). The large excess of GTP over the concentration of enzyme (approximately 30-fold), even in the presence of saturating Mg^{2+}, chelates a significant amount of Mn^{2+} such that the predominant species in solution is the Mn−GTP complex as opposed to the ternary PEPCK−Mn−GTP complex. Therefore, the observed effect is predominately from that of the binary Mn−GTP complex even in the presence of enzyme.

Table 2: Normalized Relaxation Rates of GTP Protons in the Presence of PEPCK, Mn^{2+}, and GTP[a]

	$1/pT_{1p}$ ($\times 10^3$ s^{-1})			R (Å)	
nucleus	300 MHz	500 MHz	τ_c (ns)[b]	300 MHz	500 MHz
$H_{1'}$	2.0 ± 0.5	1.8 ± 0.2	0.13	6.15 ± 0.20	6.28 ± 0.13
$H_{2'}$	20.3 ± 4.3	9.9± 3.0	0.25	4.53 ± 0.15	5.10 ± 0.33
$H_{3'}$	9.9 ± 1.5	6.5 ± 0.3	0.21	5.02 ± 0.10	5.39 ± 0.05
$H_{4'}$	nd	nd	nd	nd	nd
$H_{5',5''}$	nd	nd	nd	nd	nd
H_8	27.2 ± 2.3	23.0 ± 4.0	0.18	4.15 ± 0.06	4.27 ± 0.12
α-P[c]	1.4 ± 0.1		1.5	6.34 ± 0.09	
β-P[c]	1.8 ± 0.2		1.5	6.11 ± 0.09	
γ-P[c]	1.8 ± 0.1		1.5	6.11 ± 0.08	

[a] Relaxation rates were determined at 300 and 500 MHz; distances from the nuclei to the metal were calculated from eqs 2 and 3. [b] τ_c Determined from T_1 ratio at 300 and 500 MHz. [c] ^{31}P data from Lee and Nowak (*13*) at 121.5 MHz.

To decrease the affinity of the free nucleotide for the paramagnet, an alternative nucleotide source was investigated. The absence of β and γ phosphates in GMP significantly decreases the affinity of the ligand for metal. Binding of nucleotides to PEPCK is accompanied by a quenching of the intrinsic fluorescence of the protein at 335 nm. Titration experiments, measuring fluorescence quenching at 335 nm, (data not shown) demonstrate that GMP does bind to PEPCK with a K_D of 31 ± 2 μM, $\%Q = 17.4 \pm 0.2$. GMP is also kinetically a competitive inhibitor against GDP with a $K_I = 0.50 \pm 0.10$ mM (data not shown). The trend of decreasing the affinity of the enzyme for nucleotide with decreasing number of phosphates is observed (K_D GTP = 3.0 ± 0.5 μM, $\%Q = 18.7 \pm 0.2$, GDP = 8.0 ± 0.5 μM, $\%Q = 20.3 \pm 0.4$). The paramagnetic effect of added Mn^{2+} upon the relaxation rates of the nuclei of GMP was performed for the binary Mn−GMP complex at 600 MHz in a similar manner as for GTP (Table 3). The distances determined for

Table 3: Normalized Relaxation Rates of GMP Protons in the Binary Mn−GMP Complex[a]

nucleus	$1/pT_{1p}$ ($\times 10^3$ s^{-1})	τ_c (ns)[b]	R (Å)
$H_{1'}$	4.0 ± 0.3	0.1	5.16 ± 0.06
$H_{2'}$	11.7 ± 0.2	0.1	4.32 ± 0.02
$H_{3'}$	7.1 ± 0.3	0.1	4.68 ± 0.03
$H_{4'}$	2.8 ± 0.2	0.1	5.47 ± 0.07
$H_{5'}$	7.9 ± 0.5	0.1	4.60 ± 0.05
H_8	137.5 ± 10.7	0.1	2.86 ± 0.03
α-P[c]	5.3 ± 1.5	0.1	3.71 ± 0.15

[a] Relaxation rates were determined at 600 MHz; distances from the nuclei to the metal were calculated from eqs 2 and 3. [b] τ_c estimated from the molecular weight of the binary Mn^{2+}−GMP complex. [c] ^{31}P relaxation rates determined at 202 MHz.

Table 4: Normalized Relaxation Rates of GMP Protons in the Ternary PEPCK−Mn−GMP Complex[a]

nucleus	$1/pT_{1p}$ ($\times 10^2$ s^{-1})	$1/pT_{2p}$ ($\times 10^3$ s^{-1})	τ_c (ns)[b]	R (Å)
$H_{1'}$	0.92 ± 0.09	nd[e]	1.1	9.09 ± 0.14
$H_{2'}$	2.50 ± 0.48	nd	1.1	7.70 ± 0.22
$H_{3'}$	2.61 ± 0.30	nd	1.1	7.64 ± 0.15
$H_{4'}$	1.65 ± 0.31	3.2 ± 1.0	1.4	7.97 ± 0.20
$H_{5'}$	3.66 ± 0.52	5.6 ± 1.6	1.2	7.13 ± 0.15
H_8	4.33 ± 1.55	3.16 ± 1.0	0.8	7.35 ± 0.40
α-P[c]	16.14 ± 0.59	34.1 ± 9.5	4.3	4.53 ± 0.03 5.65 ± 0.03[d]

[a] Relaxation rates were determined at 600 MHz; distances from the nuclei to the metal were calculated from eqs 2 and 3. τ_c used is an average of τ_c from other proton resonances. [b] τ_c determined from T_1/T_2 ratio. [c] Phosphate relaxation rates determined at 202 MHz. [d] Distance calculated using the value of 1.1×10^{-9} s for τ_c. [e] ND: not determined due to multiplicity of resonances.

the binary Mn^{2+}−GMP complex are similar to those determined for the binary Mn−GTP (Table 1). The quantitation of the results of the Mn^{2+} titrations into the PEPCK−Mn^{2+}−GMP complex is summarized in Table 4. The correlation times determined from the T_1/T_2 ratio are significantly longer than those determined for the GTP experiments and are similar to values estimated from other relaxation rate studies with mPEPCK (*13*−*15*). These results suggest that the measured relaxation rates represent those for the ternary enzyme−Mn−GMP complex. The distances are also much longer than those calculated for GTP. The distance between Mn^{2+} and the α-phosphate was calculated using the correlation time estimated from the proton data since $1/pT_{2p}$ values for Mn^{2+} interactions with phosphate can include scalar effects (*13*). A temperature dependence of the relaxation rates from 5 to 35 °C shows that there is very little effect of temperature upon the longitudinal relaxation rates (data not shown). This suggests fast to intermediate exchange, which would impose the constraint that the distances calculated are at least lower limits. Additional experiments at varying concentrations of PEPCK (data not shown) demonstrate that as the enzyme concentration increases, the paramagnetic effect decreases. This suggests that the Mn^{2+}−^{1}H distances in the ternary PEPCK−Mn−GMP complex are long, >10 Å, and therefore the paramagnetic effects on the protons of the bound nucleotide are small. The paramagnetic effects seem to be manifested as a series of equilibria, and the presence of the Mn−GMP complex is still significant.

Paramagnetic Relaxation Effects of TEMPO−PEPCK upon ^{1}H Nuclei of GTP. PEPCK was derivatized with iodoacetamido-TEMPO at cys 273 as has been previously described (*15*). DTNB titrations revealed that the free cysteine content decreased from 13 to 12 after derivatization (data not shown). This modified enzyme was completely inactive. The relaxation rates of GTP protons were determined in the absence and in the presence of TEMPO−PEPCK. The observed $1/T_1$ values of GTP are shown as a function of TEMPO−PEPCK (Figure 1A). A diamagnetic control in which native PEPCK was titrated into the GTP solution was also performed. The control showed that only the $1/T_1$ of the $H_{1'}$ proton was affected by the presence of unlabeled PEPCK (Figure 1B). No other protons showed a relaxation effect due to titration with unmodified PEPCK. This was not due to any paramagnetic contamination and must be due to the introduction of an additional relaxation pathway provided to this nucleus by the protein upon binding. This effect was used to correct the $1/T_{1p}$ values for the $H_{1'}$ proton. The relaxation rates from the various nuclei of TEMPO−PEPCK bound GTP are summarized in Table 5. The correlation time for the dipolar interaction, used for distance calculations, was 1.3 ns taken from the previously determined estimates for TEMPO−PEPCK (*15*). A temperature dependence of the relaxation shows anti-Arrhenius behavior (a positive slope) indicative of fast exchange conditions (data not shown). The small frequency dependence

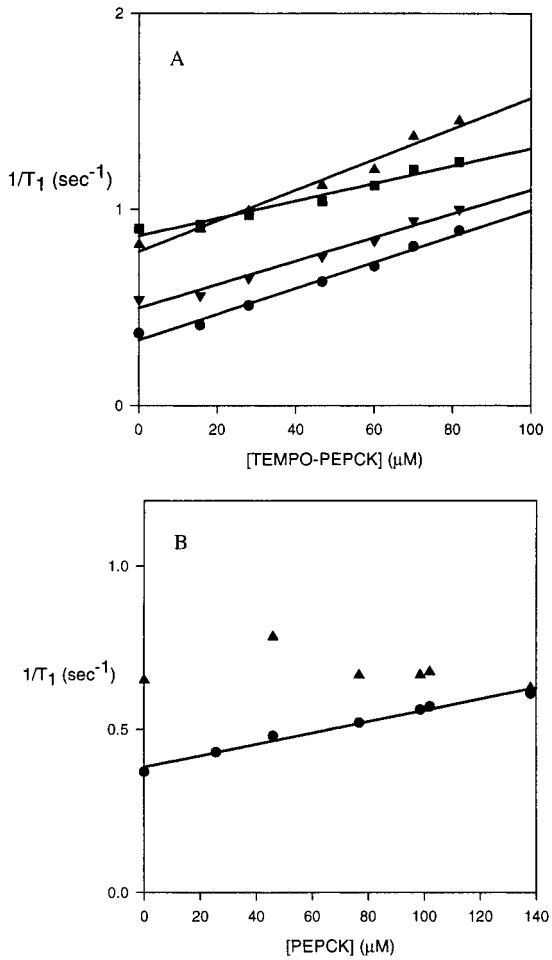

FIGURE 1: Measured $1/T_1$ values of the nuclei of GTP at 500 MHz. The $1/T_1$ values for the protons of the nucleotide $H_{1'}$ (●), $H_{3'}$ (■), $H_{4'}$ (▲), and H_8 (▼) measured as a function of added (A) TEMPO−PEPCK and (B) apo-PEPCK. In panel B, H_8 is representative of the other nuclei whose $1/T_1$ values are unaffected by the addition of PEPCK.

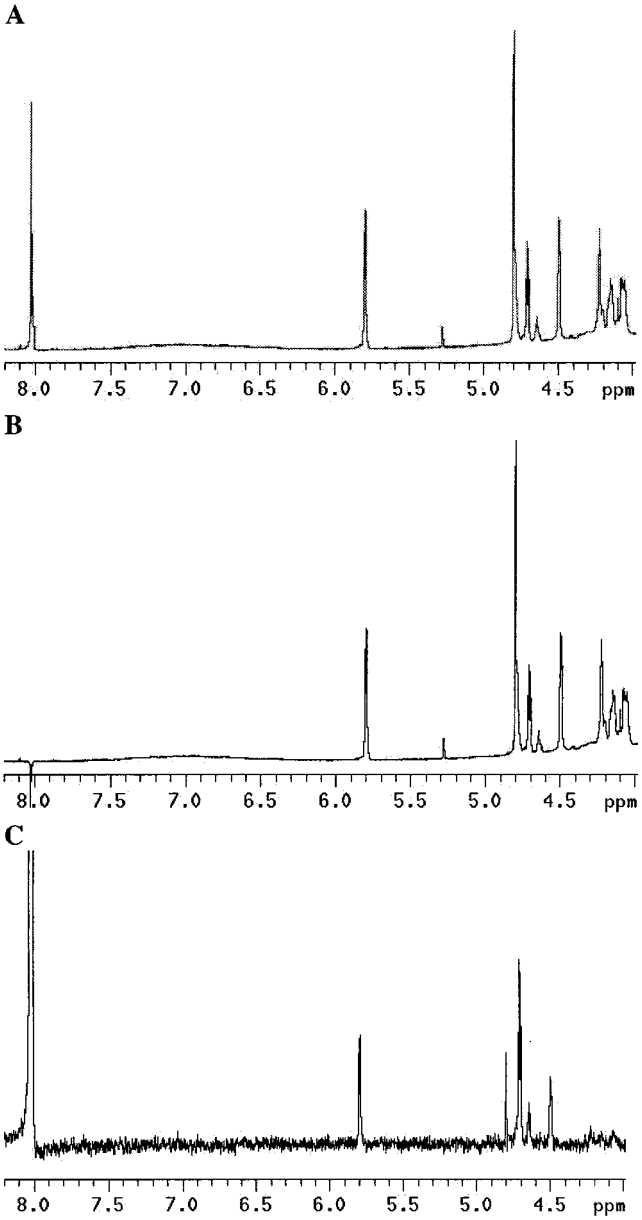

FIGURE 2: Representative nOe experiment at $\tau_m = 120$ ms. The resonance position of the nonexchangeable protons of the nucleotide are $H_{5',5''}$ (4.1 ppm), $H_{4'}$ (4.2 ppm), $H_{3'}$ (4.5 ppm), $H_{2'}$ (4.7 ppm), $H_{1'}$ (5.8 ppm), and H_8 (8.0 ppm) of the nucleotide base. The experiment was performed at 3 mM GTP, 249 μM PEPCK, 100 mM KCl, 25 mM Tris, pD 7.4, in D_2O, 10 °C. The number of transients was 144 for each spectrum. The delay time for each experiment was at least 10 times the T_1 for the proton being inverted. The spectra were acquired as described in Materials and Methods. (A) Spectrum obtained with 180° pulse at 0 ppm. (B) Spectrum obtained with 180° pulse applied to resonance corresponding to H_8 at a delay time of 120 ms. (C) Difference spectrum of (A−B) and at 10 times the vertical scale, showing the nOe's developing.

of the relaxation rates for $H_{3'}$ and H_8 also suggests fast exchange for the TEMPO−PEPCK−GTP complex.

Transferred nOe with PEPCK and GTP. Nuclear Overhauser effects on GTP that binds to PEPCK were measured. A typical nOe experiment at a single delay time is shown in Figure 2 with the selective inversion of the H_8 resonance and the developing nOe signals. nOe buildup curves for the development of nOe signals in the presence of mPEPCK (249 μM) and Mg^{2+} are shown in Figure 3. Each of the curves was fit to eq 7, and the slopes were used to determine the proton−proton coupling. These experiments were carried out at two different concentrations of mPEPCK and with the recombinant cytosolic isoform of the enzyme from rat liver (cPEPCK). The distances were calculated as outlined in Materials and Methods and are summarized in Table 6. There was no appreciable difference between the distances determined at two different concentrations of mPEPCK. The nOe buildup curves for GTP in the presence of cPEPCK had essentially the same nOe buildup rates as that shown in Figure 3.

Table 5: Normalized Relaxation Rates of GTP Protons in the Binary TEMPO−PEPCK−GTP Complex[a]

	$1/pT_{1p}$ (s^{-1})			R (Å)	
nucleus	500 MHz	600 MHz	τ_c (ns)[b]	500 MHz	600 MHz
$H_{1'}$	28.7 ± 3.0[d]	29.3 ± 3.4	1.3	5.6 ± 0.1	5.3 ± 0.1
$H_{2'}$	nd	30.5 ± 9.1	1.3	nd	5.2 ± 0.2
$H_{3'}$	18.0 ± 3.7	13.3 ± 3.7	1.3 (0.6)	6.0 ± 0.2	6.0 ± 0.3
$H_{4'}$	33.1 ± 5.1	42.4 ± 6.8	1.3	5.5 ± 0.1	5.0 ± 0.1
$H_{5',5''}$	no effect	13.6 ± 2.6	1.3		6.0 ± 0.2
H_8	24.8 ± 3.9	13.6 ± 2.1	1.3	5.7 ± 0.1	6.0 ± 0.2
α-P[c]	16 ± 4		1.3	8.7 ± 1.4	
β-P[c]	27 ± 9		1.3	7.0 ± 1.3	
γ-P[c]	22 ± 5		1.3	7.3 ± 1.3	

[a] Relaxation rates were determined at 500 and 600 MHz. ND, not determined due to spectral overlap. [b] τ_c calculated from a frequency dependence of β-P in PEPCK−ITP complex (*15*). The value in parentheses is calculated from the frequency dependence of $1/T_1$ using eq 1. [c] ^{31}P distances from Makinen and Nowak (*15*) with ITP at 121.5 MHz. [d] Observed effect not corrected for relaxation enhancement observed in the presence of unlabeled PEPCK. Corrected $1/pT_{1p}$ and r values at 500 MHz are 18.2 s^{-1} and 6.0 Å, respectively.

The distances were used as intermolecular constraints for the determination of an energy-minimized structure of the bound nucleotide. The distances determined and the bond angles for the minimized structure are tabulated in Tables 6 and 7, respectively. The pseudorotation phase angle of GTP bound to PEPCK was calculated from the bond angles in Table 7 to be 178°. The minimized structure describes a bound nucleotide molecule that has a distinct anti geometry with a χ angle of −125° [2] and the structure, calculated from these constraints, is shown in Figure 4.

Nucleotide Binding of IDP to Modified PEPCK. PEPCK was derivatized with several cysteine-specific chemical modification agents. The enzyme was desalted on a P6DG column to remove excess modification agent and the cysteine content was determined. The results are summarized in Table 8. All modified enzyme forms lost only one cysteine and retained less than 5% residual activity. The modified enzyme forms were tested for their ability to bind nucleotide by fluorescence quenching titrations. Only small differences in the K_D for IDP[3] were observed with any of the modified enzyme forms as compared with wild-type PEPCK (Table 8). There was a distinct decrease in the amount of maximal

[2] In the present work, χ is defined as $O_4'-C_1'-N_9-C_4$. Previous work has defined χ as $O_4'-C_1'-N_9-C_8$; these two values differ by 180°.

[3] Internal quenching caused by the absorption of excitation energy by higher concentrations of guanosine nucleotides complicates the determination of binding constants for the guanosine nucleotides to PEPCK by fluorescence quenching. IDP behaves identically to GDP kinetically and thermodynamically with PEPCK and does not suffer from the complication of causing quenching of the fluorescence signal.

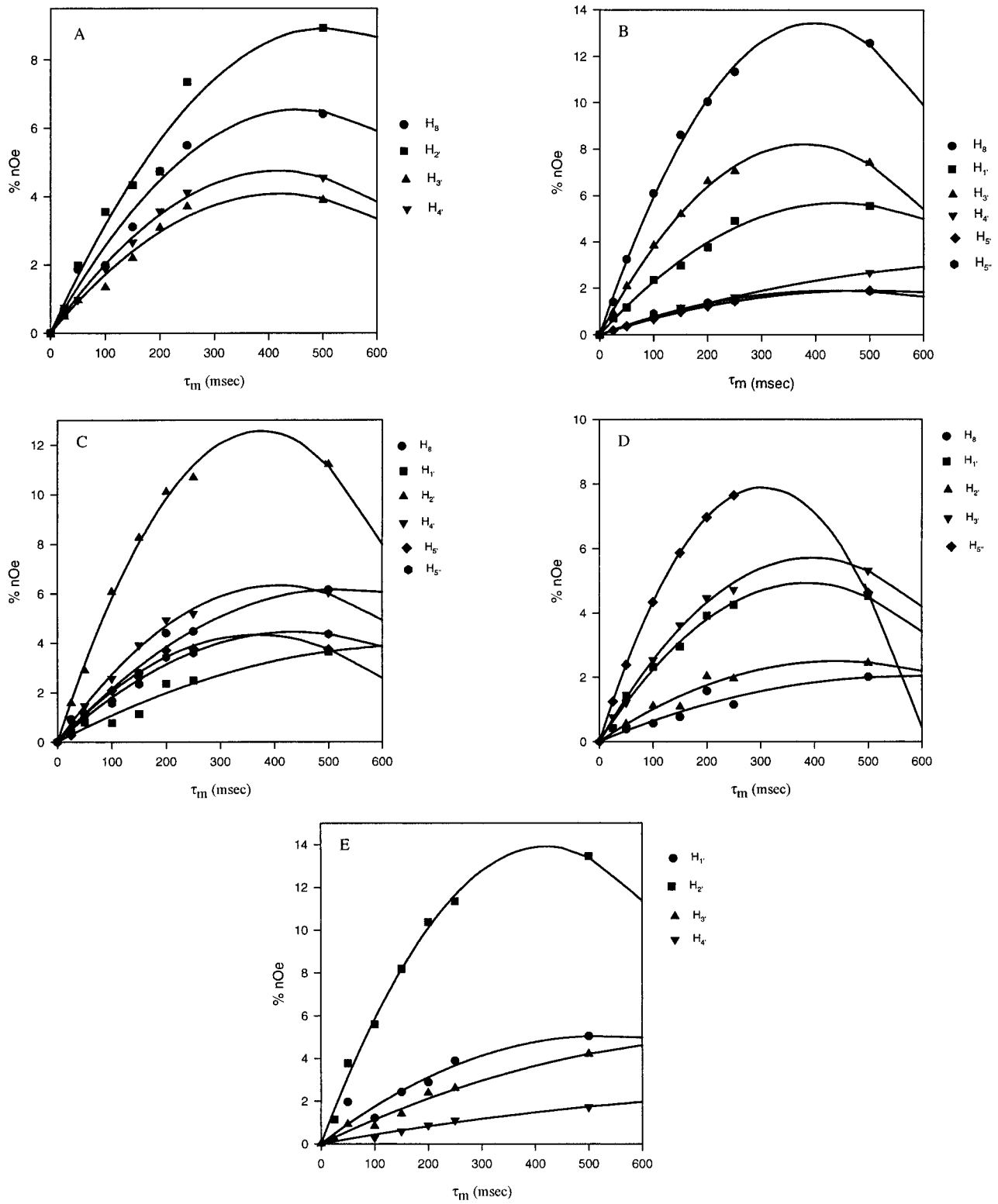

FIGURE 3: nOe buildup curves for the ^{1}H resonances of GTP in the GTP−Mg^{2+}−mPEPCK complex. The ratio of PEPCK to GTP was 1:16. Inversion of the resonance corresponding to (A) $H_{1'}$, (B) $H_{2'}$, (C) $H_{3'}$, (D) $H_{4'}$, and (E) H_8 and observation of the development of the nOe signals for each resonance is indicated in each figure.

quenching with the modified enzymes over that of wild type. The correlation between maximal quenching and the predicted length of the R group of the modified and unmodified (R = 0) cysteine residue is shown in Figure 5.

DISCUSSION

The binary complex of Mn^{2+}−GTP is similar in structure to that previously determined for the Mn^{2+}−ATP complex determined by similar techniques (*24*). The metal is presumably complexed to each of the three phosphoryl groups and has some interaction with N_7 based on the close proximity to H_8. Elimination of the two terminal phosphoryl ligands to give GMP results in a change in the coordination of the metal which has a greater interaction with the guanosine ring and a closer coordination to the nitrogen of the base (Tables 1 and 3).

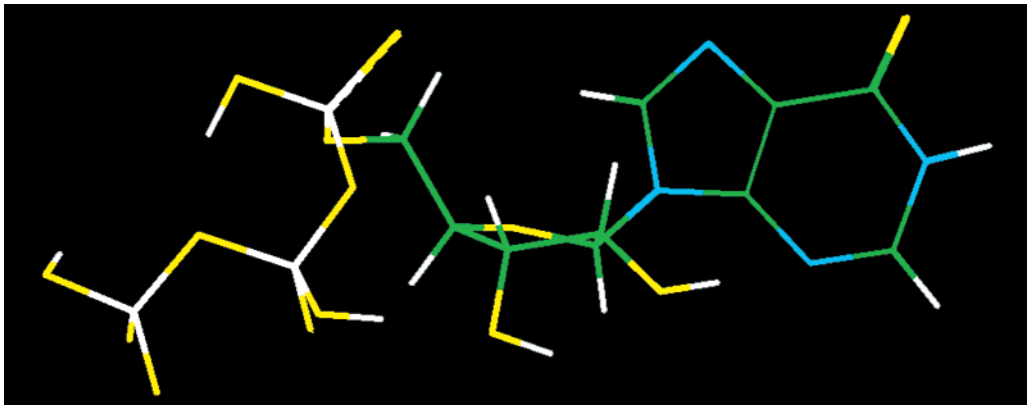

FIGURE 4: Structure of GTP bound to PEPCK as calculated using InsightII. The distance constraints utilized were those distances calculated from the nOe experiments and summarized in Table 4.

Table 6: Internuclear Distances of Bound GTP Protons[a]

	internuclear distances (Å)			
proton pairs	mPEPCK bound:free = 0.062	mPEPCK bound:free = 0.043	cPEPCK bound:free = 0.048	determined from energy minimization
$H_{1'}-H_{2'}$	2.90	2.90	2.90	2.93
$H_{1'}-H_{3'}$	3.33 ± 0.16	2.93 ± 0.02	3.16 ± 0.02	3.56
$H_{1'}-H_{4'}$	3.09 ± 0.02	2.96 ± 0.02	2.76	3.12
$H_{1'}-H_8$	3.11 ± 0.11	2.73 ± 0.10	2.63 ± 0.10	3.37
$H_{2'}-H_{3'}$	2.70 ± 0.10	2.54 ± 0.21	2.31 ± 0.08	2.23
$H_{2'}-H_{4'}$	3.62 ± 0.11	3.33	nd	3.86
$H_{2'}-H_{5'}$	3.49	3.24	nd	3.78
$H_{2'}-H_{5''}$	3.93	3.05	nd	3.88
$H_{2'}-H_8$	2.61 ± 0.01	2.34 ± 0.01	2.39 ± 0.03	2.43
$H_{3'}-H_{4'}$	2.98 ± 0.02	2.68 ± 0.15	2.61	2.80
$H_{3'}-H_{5'}$	3.06	3.02	2.82	2.72
$H_{3'}-H_{5''}$	3.18	2.71	2.67	3.51
$H_{3'}-H_8$	3.29 ± 0.18	2.69 ± 0.02	2.85	3.71
$H_{4'}-H_{5''}$	2.72	nd	nd	2.65
$H_{4'}-H_8$	3.75 ± 0.05	nd	nd	3.73

[a] Distances were determined from the initial slopes of nOe buildup curves measured with each complex; energy minimization was performed using nOe distances as constraints with an allowed deviation of 10%. The $H_{1'}-H_{2'}$ distance of 2.9 Å was used as the standard distance (*21*) from which each proton−proton distance was calculated using eq 8.

Table 7: Torsion Angles of the Energy Minimized Model of GTP Bound to PEPCK

torsion	angle (°)
χ ($O_{4'}-C_{1'}-N_9-C_4$)	−125
δ ($C_{5'}-C_{4'}-C_{3'}-O_{3'}$)	141
ν_0 ($C_{4'}-O_{4'}-C_{1'}-C_{2'}$)	−12
ν_1 ($O_{4'}-C_{1'}-C_{2'}-C_{3'}$)	27
ν_2($C_{1'}-C_{2'}-C_{3'}-C_{4'}$)	−31
ν_3 ($C_{2'}-C_{3'}-C_{4'}-O_{4'}$)	27
ν_4 ($C_{3'}-C_{4'}-O_{4'}-C_{1'}$)	−9
β ($\alpha P-O_{5'}-C_{5'}-C_{4'}$)[a]	−175
γ ($O_{5'}-C_{5'}-C_{4'}-C_{3'}$)[a]	−156
P	178

[a] Found by energy minimization only. No experimental constraints were available.

Table 8: Binding Constants and Maximal Fluorescence Quenching Values for Wild Type and Modified Forms of PEPCK

enzyme form	cysteine/ enzyme	K_D IDP (μM)	% Q_{max}
wild type	12.8 ± 0.3	79 ± 6	16.2 ± 0.4
iodoacetamide	12.2 ± 0.2	53 ± 7	5.6 ± 0.2
iodoacetate	12.1 ± 0.3	31 ± 2	9.9 ± 0.2
MMTS	11.7 ± 0.3	110 ± 13	7.6 ± 0.3

Previous ^{31}P studies of GTP binding to PEPCK−Mn^{2+} indicate that the nucleotide phosphates exist in an extended chain conformation oriented toward the active site metal (*13*). Experiments performed to determine the orientation of the nucleotide portion of the molecule with respect to the active site metal generates inconclusive results (Tables 2 and 4). This is apparently due to the long distances that are present between the metal and the protons of the ribose and nucleotide rings that result in very small relaxation effects. Upon the basis of the $Mn^{2+}-^{31}P$ distances reported (*13*, *14*), the closest distance to the Mn^{2+} would be that of $H_{5'}$, which is estimated to be on the order of 9 Å. The data, although inconclusive, is consistent with the base of the active site nucleotide oriented away from the bound Mn^{2+} which is closest to the gamma phosphate of GTP. This is expected if Mn^{2+} plays a key role in the mechanism of transfer of the γ-phosphate from GTP to OAA. These long $Mn^{2+}-^1H$ dipolar distances, coupled with the propensity to form Mn^{2+}−nucleotide binary complexes even in the presence of enzyme, lead to the indeterminate relaxation rate measurements for the PEPCK−Mn−GTP complexes. The PEPCK−Mn^{2+}−GTP population would be expected to have greater Mn^{2+}−proton distances than for those in the binary Mn^{2+}−GTP complex. The paramagnetic effects are dominated by the shorter dipolar distances in the binary complex due to the r^6 dependence in the Solomon−Bloembergen equation (eq 2).

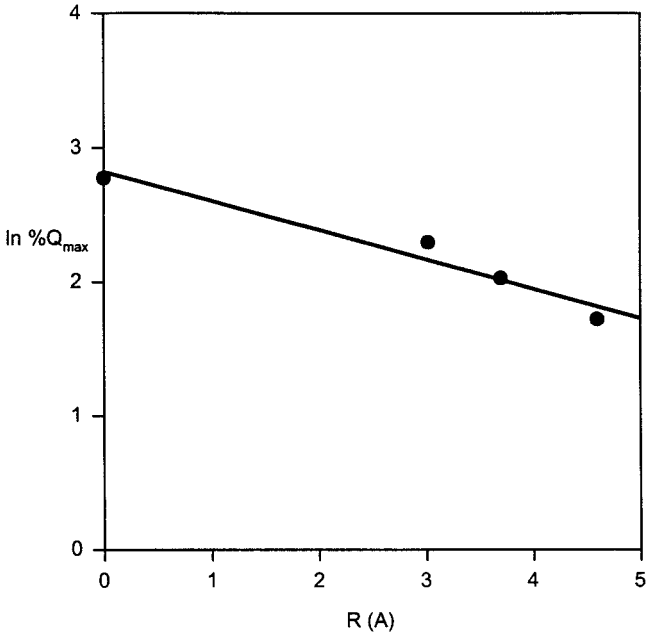

FIGURE 5: Maximal fluorescence quenching as a function of the extension of the cys273 side chain. PEPCK was modified as described in Materials and Methods and titrated with nucleotide. The agents used were iodoacetate (3.0 Å) and MMTS (3.7 Å) and iodoacetamide (4.6 Å). The resulting titration curve was fit to maximal quenching as a function of the length of the modifying group R. The value for R was estimated from model building.

From the model of the GTP structure at the active site (Figure 4), obtained from the nOe experiments and energy minimization calculations (Tables 6 and 7), and by locating the Mn^{2+} relative to the polyphosphate chain of GTP (*13*), distances from the Mn^{2+} to protons of GTP can be estimated. From these estimates, values for $1/pT_{1p}$ from 80 to 150 s^{-1} are calculated. These are well below the sensitivity of these experiments. Previous studies measuring ^{31}P relaxation effects have suggested that GTP is in fast exchange with PEPCK−Mn (*13*). The weaker binding ligand GMP is also expected be in fast exchange. Slow exchange phenomena for $Mn^{2+}-{}^{1}H$ interactions would be due to small relaxation effects by PEPCK−Mn to protons that are a long distance away. The ^{1}H relaxation rates for the PEPCK−Mn−GMP complexes may be in intermediate exchange. The data summarized in Table 4 indicate the base of the nucleotide faces away from the Mn^{2+} and H_8 points toward the Mn^{2+} in an anti configuration.

The results of the transient nOe experiments are consistent with an anti conformation of the GTP nucleotide bound to PEPCK. Both the chicken mitochondrial and the rat cytosolic isoforms of PEPCK yield similar internucleotide distances. The nOe buildup curves for the lower concentrations of mPEPCK and cPEPCK are similar to those shown in Figure 3. The torsion angle χ of −125° is similar to that measured in many other systems where bound nucleotides have been determined to be in an anti conformation. All of these complexes exhibit χ angles of approximately −130° (*20*, *25*−*29*). The angle determined is also consistent with the classical definition of an anti geometry in which $-90° \leq \chi \geq -160°$ (*21*). The pseudorotation phase angle *P* is used as a measure of the pucker of the sugar moiety of a nucleotide (*21*). The calculated *P* for GTP bound to PEPCK (178°) is consistent with ^{2}E puckering of the ribose ring (*21*). The torsion angle ν_4 (−9°) is close to 0°, which defines a ribose ring that has a classic envelope $C_{2'}$-endo (^{2}E) conformation (*21*, *29*). This conformation is in direct contrast with the structure of the bound nucleotide (ATP) determined crystallographically for the *E. coli* isoform (*12*). This structure, cocrystallized with ATP and oxalate, shows the nucleotide in a syn conformation with a χ angle of 57.5° (*11*, *12*). This conformational variation may reflect a key difference in the mechanisms by which the *E. coli* ATP-utilizing isoforms and the GTP class of PEPCKs catalyze similar reactions. It has been suggested that GTP- and ATP-utilizing PEPCKs, although exhibiting little overall sequence identity, have conserved nucleotide binding motifs (*11*). The different conformations of the bound nucleotide argue against this suggestion. Further support against the generalized binding motif comes from the preparation of a catalytically competent Co^{3+}−PEPCK complex and the elucidation of active site metal ligands as being asp295 and asp296 (*30*, *31*). While the respective amino acids, asp268 and 269, in the *E. coli* structure are shown to be metal ligands, they were proposed to interact through two water molecules in the coordination sphere of the nucleotide metal and not the activating metal site (*11*, *12*). The conformation of GTP determined here is remarkably similar to the conformation of bound nucleotide in IMP dehydrogenase determined by similar techniques (*29*). In that study, the ribose ring was found to have a similar envelope $C_{2'}$-endo (^{2}E) conformation ($P = 166°$, $\nu_4 = -2°$), and a χ angle of −123°. The ability of inosine nucleotides to adopt a similar conformation to guanosine nucleotides agrees with the ability of PEPCK to use both classes of purines as substrates.

PEPCK has been shown to contain one reactive cysteine that, upon chemical modification, leads to inactivation of the enzyme (*15*). On the basis of binding studies to modified enzyme and on studies with spin-labeled enzyme where the label was on the reactive cysteine, it was proposed that this residue is not actively participating in catalysis due to its remoteness from the active site Mn^{2+}. Protection from inactivation was provided by nucleotide. This led to the hypothesis that perhaps cys273 directly interacts with the bound nucleotide. GTP binds to TEMPO−PEPCK and measurements of the effect of the nitroxide of the TEMPO-derivatized PEPCK with the protons and phosphates of GTP result in distances that are too long to involve direct interaction between the cys273 thiol side chain and the bound nucleotide. This conclusion is supported by recent pH studies that show cys273 ionization occurs with an apparent pK_a of 8.0. No pK_a value for this ionization appears in the k_{cat} or k_{cat}/K_{Mg-IDP} profiles (*32*). The binding of nucleotide to PEPCK has also been shown to be pH independent over the pH range of 6.5−9 indicating that the ionization state of cys273 bears no impact upon nucleotide association (Holyoak and Nowak, unpublished results). Further evidence is provided by the steady state fluorescence quenching experiments. There is no significant change in the affinity of the derivatized forms of the enzyme for nucleotide regardless of the side chain charge or length of the modifying agent attached to cys273 (Table 8). The closest approach of the nitroxide of TEMPO, which is already lengthened approximately 7 Å over that of the native cysteine side chain is 5.3 Å. This provides a distance constraint that is too long for direct interaction of the cys273 side chain with the

nucleotide ribose. The fluorescence experiments suggest an alternative role for cys273. While all derivatized forms of the enzyme bind nucleotide with comparable affinities to wild-type PEPCK, the maximal quenching that is observed upon saturation of the enzyme with nucleotide decreases with the apparent increase in chain length of the chemical modifier. This suggests that the cysteine may be in a hinge region between two domains of the enzyme that must close to facilitate phosphoryl transfer between GTP (GDP) and OAA (PEP). The crystal structure of *E. coli* PEPCK shows that the enzyme consists of two distinct domains (*10*, *11*). A similar general structure may exist for avian PEPCK. Upon nucleotide binding to avian PEPCK, a significant amount of fluorescence quenching (16%) is observed. This is presumably the result of a conformational change that occurs upon nucleotide binding that closes the active site and allows for phosphoryl transfer. Evidence for a domain closure was also seen in the *E. coli* crystal structure. A rather large domain movement was observed in the crystal structure of *E. coli* PEPCK between the apo structure and that cocrystallized with ATP and oxalate. The structure determined in the presence of oxalate and ATP showed a 20° movement of the N-terminal domain toward the C-terminal domain upon nucleotide binding (*11*). The observed quenching of avian mPEPCK is similar to results with *E. coli* PEPCK where approximately 16% quenching upon titration with ATP is measured (*33*). As compared to IDP quenching of wild-type PEPCK, all the modified enzyme forms show a significant decrease in the maximal quenching achieved upon saturation with nucleotide (Table 8). This value varies among the agents used. Figure 5 shows that there appears to be a direct correlation between the length of the modified cysteinyl side chain and the amount of quenching observed. One interpretation of the data is that as the side chain on cys273 is lengthened beyond that present in the wild-type enzyme, the active site is no longer able to completely close and allow for efficient transfer of the phosphoryl group of GTP. This interpretation is consistent with the previous nitroxide−metal distances (*15*), the nitroxide−^{1}H distances presented here, and the pH dependence studies (*32*) that argue against inactivation through modification of a critical active site residue. The nitroxide−^{1}H distances also argue against a role for cys 273 in binding. This is also supported by the steady-state fluorescence experiments in which the K_D for nucleotide is not affected upon side chain modification. Mutagenesis of the reactive cysteine with both the rat cytosol and *Ascaris suum* forms of PEPCK reveal that while k_{cat} is reduced on the order of 2−3-fold, the mutants of the corresponding cysteine residue are catalytically active and bind nucleotide with wild type affinity (Holyoak & Nowak and Rios & Nowak, unpublished observations). Ultimately the role of cys273 will have to be clarified with the crystal structures of the apo enzyme and the nucleotide complexes.

The observation from the TEMPO experiments that a relaxation enhancement of the $H_{1'}$ proton of GTP occurs upon enzyme binding is interesting. This observation suggests a direct interaction of a protein ligand with the nucleotide. Since the $H_{1'}$ proton is substantially spin isolated, it is sensitive to additional relaxation pathways. A specific hydrogen bond at this location is suggested by these results.

Upon the basis of the differences in the nucleotide conformations determined for GTP and for ATP-utilizing classes of PEPCK, it is feasible that key differences in the way the two types of enzymes catalyze similar reactions revolves around the nucleotide and its binding site. Both classes have a common mechanism by which nucleotide triggers domain closure thus excluding water from the active site (*11*). Closing of the active site would be necessary to prevent futile hydrolysis of the triphosphate nucleotide rather than efficient phosphoryl transfer which is intrinsic to the PEPCK catalyzed mechanism.

ACKNOWLEDGMENT

The authors express their appreciation for the assistance of Dr. Jaroslav Zajicek for assistance with the nOe experiments.

REFERENCES

1. Utter, M. F., and Kurahashi, K. (1953) *J. Am. Chem. Soc. 75*, 758.
2. Valera, A., Pujol, A., Pelegrin, M., and Bosch, F. (1994) *Proc. Natl. Acad. Sci. U.S.A. 91*, 9151−9154.
3. Weldon, S. L., Rand, A., Matathias, A. S., Hod, Y., Kalonick, P. A., Savon, S., Cook, J. S., and Hanson, R. W. (1990) *J. Biol. Chem. 265*, 7308−7317.
4. Nordlie, R. C., and Lardy, H. A. (1963) *J. Biol. Chem. 238*, 2259−2263.
5. Chiao, Y. (1976) *The Intracellular Localization and Kinetic Properties of Chicken Liver Phosphoenolpyruvate Carboxykinase.* Ph.D. dissertation, Case Western Reserve University.
6. Gevers, W. (1967) *Biochem. J. 103*, 141−152.
7. Holten, D. D., and Nordlie, R. C. (1965) *Biochemistry 4*, 723−731.
8. Wieldland, O., Evertz-Prusse, E., and Strukowski, B. (1968) *FEBS. Lett. 2*, 26−28.
9. Brech, W., Shrango, E., and Wilken, D. (1970) *Biochim. Biophys. Acta 201*, 145−154.
10. Matte, A., Goldie, H., Sweet, R. M., and Delbaere, L. T. J. (1996) *J. Mol. Biol. 256*, 126−143.
11. Matte, A., Tari, L., W., Goldie, G., and Delbaere, L., T., J. (1997) *J. Biol. Chem. 272*, 8105−8108.
12. Tari, L., W., Matte, A., Goldie, H., And Delbaere, L., T., J.-(1997) *Nat. Struct. Biol. 4*, 990−994.
13. Lee, M. H., and Nowak, T. (1984) *Biochemistry 23*, 6506−6513.
14. Duffy, T., and Nowak, T. (1985) *Biochemistry 24*, 1152−1160.
15. Makinen, A. L., and Nowak, T. (1989) *J. Biol. Chem.* 264, 12148−12157.
16. Hebda, C. A., and Nowak, T. (1982a) *J. Biol. Chem. 257*, 5503−5514.
17. Fersht, A. (1985) in *Enzyme Structure and Mechanism*, 2nd ed., p 33, W. H. Freeman and Company, New York.
18. Solomon, I. (1955) *Phys. Rev. 99*, 559−565.
19. Nowak, T.(1981) in *Spectroscopy in Biochemistry* (Bell, J. E., Ed.) Vol II, pp 109−135, CRC Press Inc., Boca Raton, FL.
20. Jarori, G. K., Murali, N., Switzer, R. L., and Rao, B. D. N. (1995*) Eur. J. Biochem. 230*, 517−524.
21. Saenger, W. (1984) in *Principles of Nucleic Acid Structure* (Cantor, C. R., Ed.) pp 9−28, Springer-Verlag, New York.
22. Habeeb, A., F., S. (1972) *Methods Enzymol. 25*, 457−464.
23. Lee, M. H., Hebda, C. A., and Nowak, T. (1981) *J. Biol. Chem. 256*, 12793−12801.
24. Sloan, D. L., and Mildvan, A. S. (1976) *J. Biol. Chem. 251*, 2412−2420.
25. Frick, D., N., Weber, D. J., Abeygunawardana, C., Gittis, A., G., Bessman, M., J., and Mildvan, A., S. (1995) *Biochemistry, 34*, 5577−5586.

26. Murali, N., Jaori, G., K., Landy, S., B., and Rao, B., D. (1993) *Biochemistry 32*, 12941−12948.
27. Murali, N., Jarori, G., K., and Rao, B., D. (1994) *Biochemistry 33*, 14227−14236.
28. Jarori, G. K., Murali, N., and Rao, B., D. (1994) *Biochemistry 33*, 6784−6791.
29. Xiang, B., and Markham, G., D. (1996) *J. Biol. Chem*. *271*, 27531−27535.
30. Hlavaty, J. J., and Nowak, T. (1997) *Biochemistry 36*, 3389−3403.
31. Hlavaty, J. J., and Nowak, T. (1997) *Biochemistry 36*, 15514−15525.
32. Holyoak, T., and Nowak, T. (2001), to be submitted.
33. Encinas, M. V., Rojas M. C., Goldie, H., and Cardemil, E. (1993) *Biochim. Biophys. Acta 1162*, 195−202.

BI011374N